Total Synthesis of Photoactivatable or Fluorescent Anandamide Probes: Novel Bioactive Compounds with Angiogenic Activity

Laurence Balas,*[,†] Thierry Durand,[†] Sattyabrata Saha,[‡] Inneke Johnson,[‡] and Somnath Mukhopadhyay[‡,§]

Institut des Biomolécules Max Mousseron (IBMM), UMR 5247 CNRS, Université de Montpellier I and Université de Montpellier II, 15, Av. Ch. Flahault, F-34093 Montpellier Cedex 05, France, Neuroscience Research Program, JLC-Biomedical Biotechnology Research Institute, North Carolina Central University, 700 George Street, Durham, North Carolina 27707, and Department of Chemistry, Division of Biochemistry, North Carolina Central University, Durham, North Carolina 27707

Received September 11, 2008

Endocannabinoids are endogenous polyunsaturated fatty acids involved in a multitude of health and disease processes. Recently, several lines of evidence suggest the presence of a novel non-CB1/CB2 anandamide receptor in endothelial cells. Thus, we synthesized two types of photoaffinity probes that contain either an arylazide group or a diazirin moiety, together with a fluorescent analogue. The key steps rely on selective hydrogenation of skipped tetrayne backbones and on copper-mediated cross-coupling reactions between diynic precursors. Three synthetic routes were investigated. In biological functional assays, we found that both the arylazide and the fluorescent probes induced robust increases in matrix metalloprotease activity and produced positive angiogenic responses in in vitro endothelial cell tube formation assays. Irradiation of the arylazide probe nicely enhanced this effect in both HUVEC and CB1-KO HUVEC. These results suggest that the arylazide and the fluorescent probes can be used to identify "non-CB1/CB2 anandamide receptor" from endothelial cells.

Introduction

Endocannabinoids (eCBs[a]) are a family of endogenous polyunsaturated long-chain fatty acid (PUFA) derivatives,[1] regarded as promising templates for the development of new pharmacological agents potentially useful for various conditions. The first eCB to be discovered[2] was the ethanolamide of arachidonic acid (also called anandamide). The seven eCBs isolated to date are shown in Figure 1, together with four structurally related endogenous lipoamino acids (also called elmiric acids[3]), i.e., NAala, NAgly, NAGABA, ARA-S, and a taurine derivative NAT.[4−6] All of these newly isolated PUFA derivatives are known to exist in brain tissue and appear to exhibit properties similar to anandamide. However, little or no information is currently available concerning their natural occurrence or biological roles.

The therapeutic potential of agents that influence the eCB system is impressive. Abundant evidence indicates that eCBs participate as neuromodulators in numerous physiological and/or pathological processes.[7−9] Besides their involvement in chronic pain, other conditions where abnormal activity of the eCB system has been implicated include neurological/psychological disorders (multiple sclerosis, Alzheimer's disease, Parkinsonism, schizophrenia, epilepsy, learning and memory deficits, anorexia) as well as cardiovascular disease states (hypertension, atherosclerosis), AIDS, and intestinal disorders. It is well established that the eCBs bind to the same GPCR receptors (i.e., CB1 and CB2)[10] as phytocannabinoid drugs such as Δ^9-tetrahydrocannabinol (THC), the principal psychoactive agent in the *Cannabis sativa* plant. Depending on their structures and localization, the eCBs may exert very different effects on CB1 and CB2 receptors, acting[11] as partial agonists, full agonists, or antagonists. Moreover, these receptors have a widespread distribution in various tissues and organ systems.[12] Several excellent reviews on the biochemistry and pharmacology of eCBs have appeared in recent years[12−17] Nevertheless, many questions remain unanswered. In fact, the more the eCB system is studied, the more complex it appears,[18] leading some authors[19] to call it "the eCB soup".

Interestingly, in transgenic CB1 knockout and CB1/CB2 double knockout mice, anandamide produces biological responses that must be attributed to alternative pharmacological targets other than the identified cannabinoid receptors. Multiple lines of evidence suggest the existence of several types of non-CB1/CB2 receptors in different tissues.[20−25]

To date, none of these putative receptors have been isolated or cloned. However, recent findings from our laboratories have shown that anandamide analogue methanandamide acting on this non-CB1/CB2 anandamide receptor can activate angiogenic responses in endothelial cells.[26,27] In those studies we have also illustrated that methanandamide acting on non-CB1/CB2 anandamide receptors stimulates eNOS protein to produce nitric oxide in endothelial cells.[28,26]

Clearly, pharmacological studies of the eCB system would benefit from the availability of tools that would assist in the detection, isolation, and characterization of these putative receptors. Fluorescent[29] and photolabeling[30] techniques are widely used for mechanistic studies of receptors and their binding properties and might provide interesting information on the eCB system. Fluorescence microscopy can reveal the exact location of the target protein. Photoaffinity labeling of

* To whom correspondence should be addressed. Phone: +33-4-67-54-86-24. Fax: 33-4-67-54-86-25. E-mail: balas@univ-montp1.fr.

† Université de Montpellier.

‡ JLC-Biomedical Biotechnology Research Institute, North Carolina Central University.

§ Division of Biochemistry, North Carolina Central University.

[a] Abbreviations: AcOH, acetic acid; AIDS, acquired immune deficiency syndrome; bFGF, fibroblast growth factor; BSA, bovine serum albumin; CB, cannabinoid; DMF, dimethylformamide; eCB, endocannabinoid; EDTA, ethylenediaminetetraacetic acid; FBS, fetal bovine serum; GPCR, G-protein-coupled receptor; HFIP, hexafluoroisopropanol; HUVEC, human umbilical vein endothelial cells; KO, knockout; MMP, matrix metalloproteinase; PUFA, polyunsaturated fatty acid; SN, nucleophilic substitution; TBAF, tetrabutylammonium fluoride; TBDPS, *tert*-butyldiphenylsilyl; TBMB, 2-*tert*-butyl 2-methyl-1,3-benzodioxole-4-carboxylate; THC, Δ^9-tetrahydrocannabinol; THF, tetrahydrofuran; TIMP, tissue inhibitor of metalloprotease.

10.1021/jm8011382 CCC: $40.75
Published on Web 01/22/2009

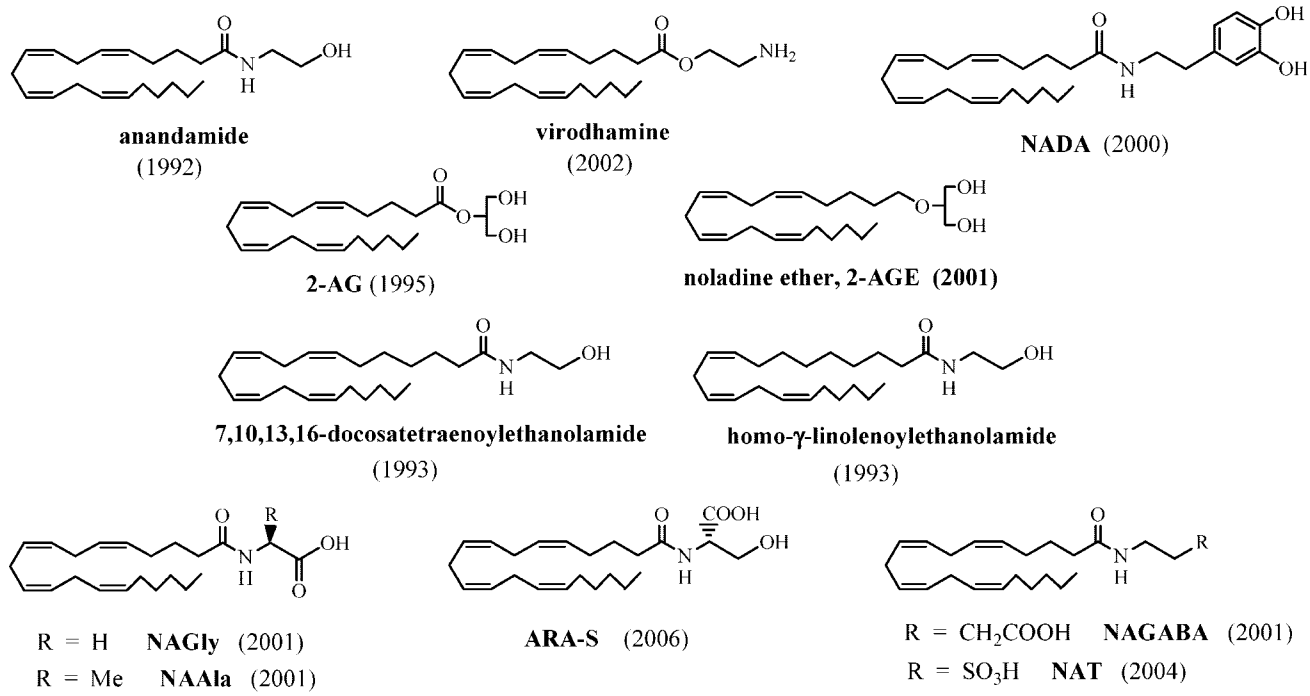

Figure 1. Endogenous ligands discovered to date.

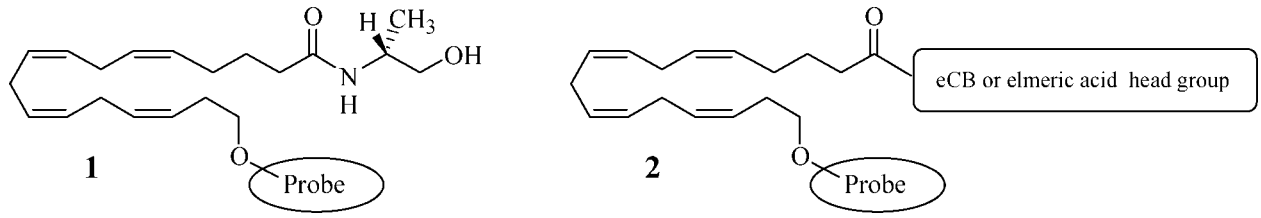

Figure 2. Targeted compounds.

receptors is particularly useful for the isolation of putative receptors. In this case, the receptor is tagged with an irreversible ligand, formed when the ligand is converted to a highly reactive species, e.g., a nitrene or carbene[31] by photoactivation. These reactive "suicide" agonists or antagonists insert covalently into C−H or O−H bonds of the closest amino acids in, or near, the binding pocket of the putative receptor protein.

We synthesized a replica of the anandamide structure with C-methylation, as a relatively minor structural modification of the polar headgroup and the inclusion of a photoreactive probe on the tail region of the analogue **1** (Figure 2). It is noteworthy that one of the shortcomings of anandamide as an effective pharmacological tool is its rapid in vivo and in vitro degradation. Methylation at the α-position of the nitrogen atom is known to result in a compound more resistant to enzymatic degradation, i.e., the analogue *R*-(+)-methanandamide.[32] Concerned with possible steric hindrance[33] and interference with the "horseshoe" conformation of the PUFA backbone, the pentyl chain was shortened to an ethylene group. In our preliminary paper,[34] we reported the synthesis of a new anandamide arylazide probe. Herein, we report the details of its synthesis as well as those of three novel probes **1** that bear either a diazirin photoactivatable or a fluorescent group at the terminus of the anandamide lipophilic chain.

We further tested the ability of these compounds to stimulate angiogenesis as a biological function triggered by the activation of non-CB1/CB2 anandamide receptors in endothelial cells to verify the validity of these probes as specific non-CB1/CB2 anandamide receptors. Our design represents a flexible synthetic strategy that allows the facile modification of head and/or tail groups at a later stage (analogues **2**).

Results and Discussion

Our retrosynthetic strategy (Scheme 1) relies on the esterification of the hydroxy function on the tail of the key tetraene intermediate **3b** with photoreactive carboxylic acids. The four skipped cis-double bonds come from selective hydrogenation of a tetrayne derivative **4**. Instead of the previously described linear strategy[35,36] that built consecutively the diyne, triyne and then tetrayne backbone, we developed a convergent route to tetrayne **4** by coupling the two skipped diynes **5** and **6**. This has the advantage, over the linear strategy, of requiring fewer experimental steps with these unstable structures. Each skipped diyne comes from organometallic cross-coupling reactions between commercially available terminal alkynes and propargylic halides.

As outlined in Scheme 1, three routes were investigated: the eCB (and elmiric acid) headgroup may be introduced after sensitive elaboration of the tetraene backbone (pathway A) or from the very beginning of the synthesis (pathway B). Therefore, tetraene **3a** (pathway A) will serve as a pivotal intermediate to obtain analogues **2** with different eCB head groups and different photoreactive tail groups whereas pathway B focuses on one eCB series only (herein, anandamide analogues **1**).

Replacement of one alkyne function in the tetrayne key intermediate **4** with a Z-alkene function was investigated (pathway C) to confer greater chemical stability to the intermediate **7**.

Scheme 1. Retrosynthetic Analysis

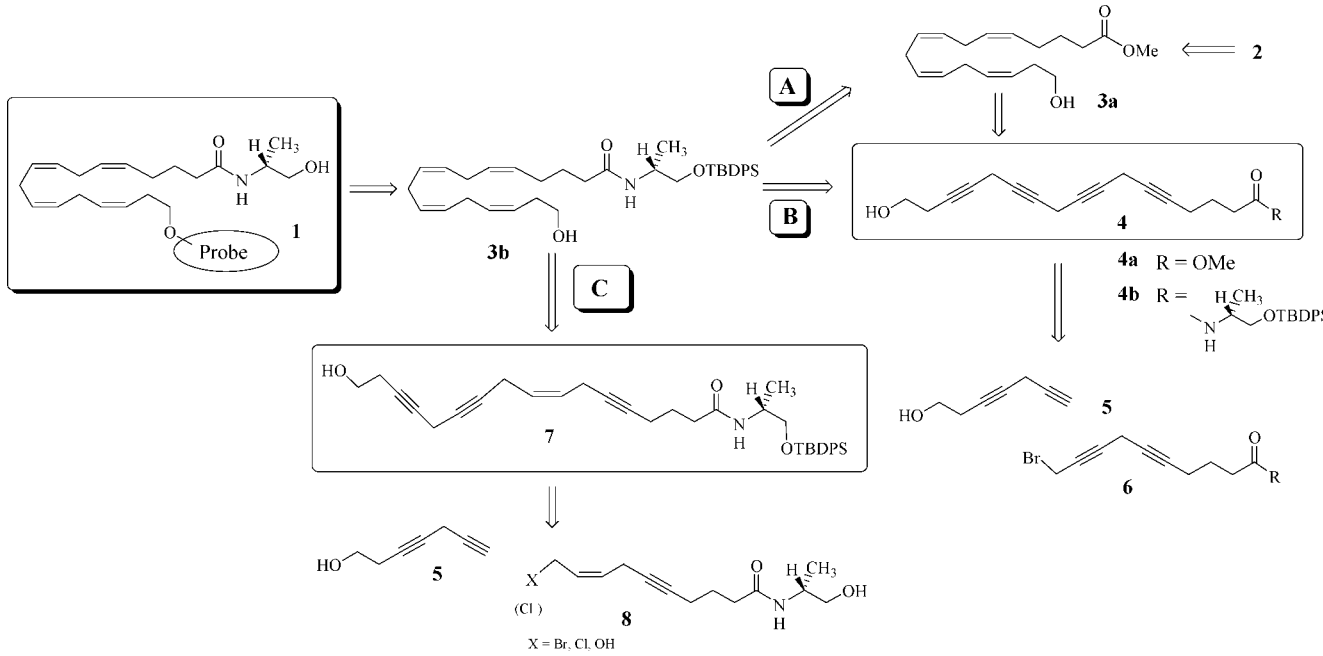

Scheme 2. Synthesis of Terminal Alkyne

	5 / 12	collected yield
TBAF, THF, O °C	2 / 98	quant.
KOH, EtOH	1 / 99	quant.
$AgNO_3$, base, EtOH	40/ 60	50%
TBAF, AcOH, THF, -8 °C	100/0	95-99%

Pathway A. The diyne precursor **5** was prepared in two steps with excellent yield (95%, Scheme 2) by means of a copper-mediated cross-coupling reaction between the commercially available 3-butyn-1-ol **9** and 3-bromo-1-(trimethylsilyl)-1-propyne **10**, followed by deprotection of the masked terminal alkyne. Upon flash chromatography (required to remove salts, starting materials, and remaining DMF), the silylated diyne **11** is recovered as a mixture with its deprotected analogue **5** (about 5−10%). The partial deprotection at this stage was not considered a problem, since the next step resulted in complete conversion of **11** to **5**. This last step was initially problematic, since the terminal diyne **5** readily rearranges to its corresponding allene **12** on silica or Florisil solid phase columns and under basic conditions. Thus, standard C−Si deprotection with fluoride ions, aqueous alcoholic potassium hydroxide, or silver nitrate mainly led to the allene structure **12** (Scheme 2). Addition of acetic acid simultaneously to the tetrabutylammonium fluoride in order to reach complete neutrality was required in order to obtain pure terminal diyne **5** in high yield (95−99%).

Starting from the commercially available 5-hexynoic acid **13**, the bis-propargylic bromide **6a** was obtained in three steps (Scheme 3) according to the procedure reported by Razdan.[37]

As depicted in Scheme 3, a subsequent cross-coupling reaction between the two precursors **5** and **6a** using Caruso conditions[38] afforded the tetrayne **4a**. It is advisable to carry out the transformation of tetrayne **4a** to tetraene **3a** on the same experimental day, as **4a** deteriorates on standing. Attempts to further repurify the sample will then be pointless. The selective hydrogenation step was performed under the Ni-P2 conditions with only moderate yield, reflecting the poor stability of the starting tetrayne **4a**. After protection of the homoallylic alcohol with a dimethoxytrityl group and saponification with lithium hydroxide in methanol, the resulting carboxylic acid **15** was coupled with di-*O*-*tert*-butyldiphenylsilyl-L-alaninol **16** to give the amide **17** using the anhydride activation procedure. We suggest that ethanolamine **16** can be replaced with any primary amine function to incorporate the other eCB or elmiric acid head groups, provided their functionalities are suitably protected. Subsequently, removal of the dimethoxytrityl group using the acidic properties of hexafluoroisopropanol (HFIP)[39] afforded the expected key alcohol **3b** in good yields.

Pathway B. As explained above, the aim of our program is to investigate the existence of new anandamide receptors. Thus, we initially focused our attention on the synthesis of various anandamide analogues. To this end, the ethanolamide headgroup was introduced at the very beginning of the synthesis, which avoided the homoallylic alcohol protection−deprotection steps.

The shortened strategy is depicted in Scheme 4. Thus, the skipped tetrayne backbone **4b** was reached in four steps only, consisting of amide bond formation between the amine **16** and 5-hexynoic acid **13**, followed by a copper cross-coupling reaction with propargylic chloride[40] **19**, bromination, and a copper cross-coupling reaction between the resultant bis-propargylic bromide **6b** and the terminal diyne **5**. As observed

Scheme 3. Synthesis of Tetraene **3b** via Tetraene **3a**

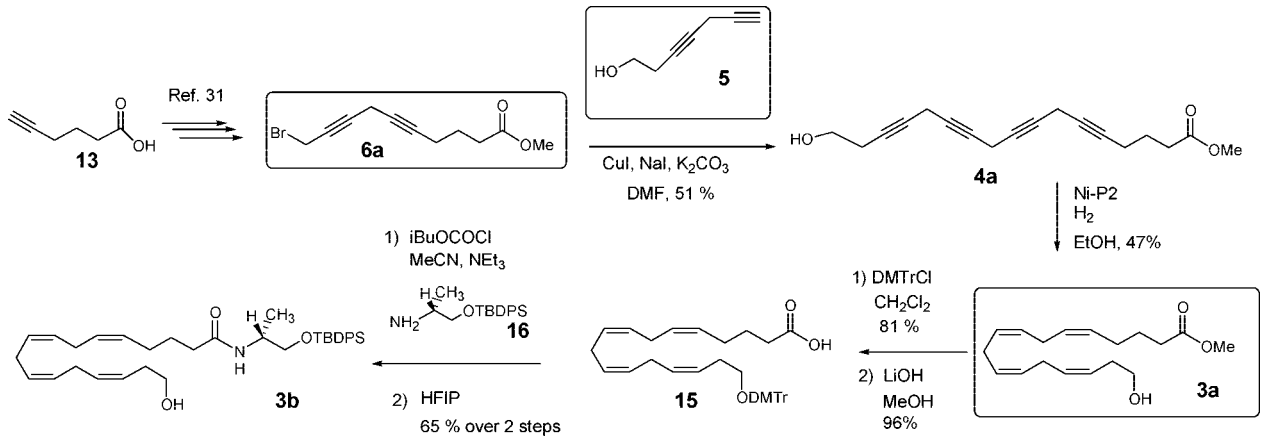

Scheme 4. Shorter Synthesis of Tetraene **3b**

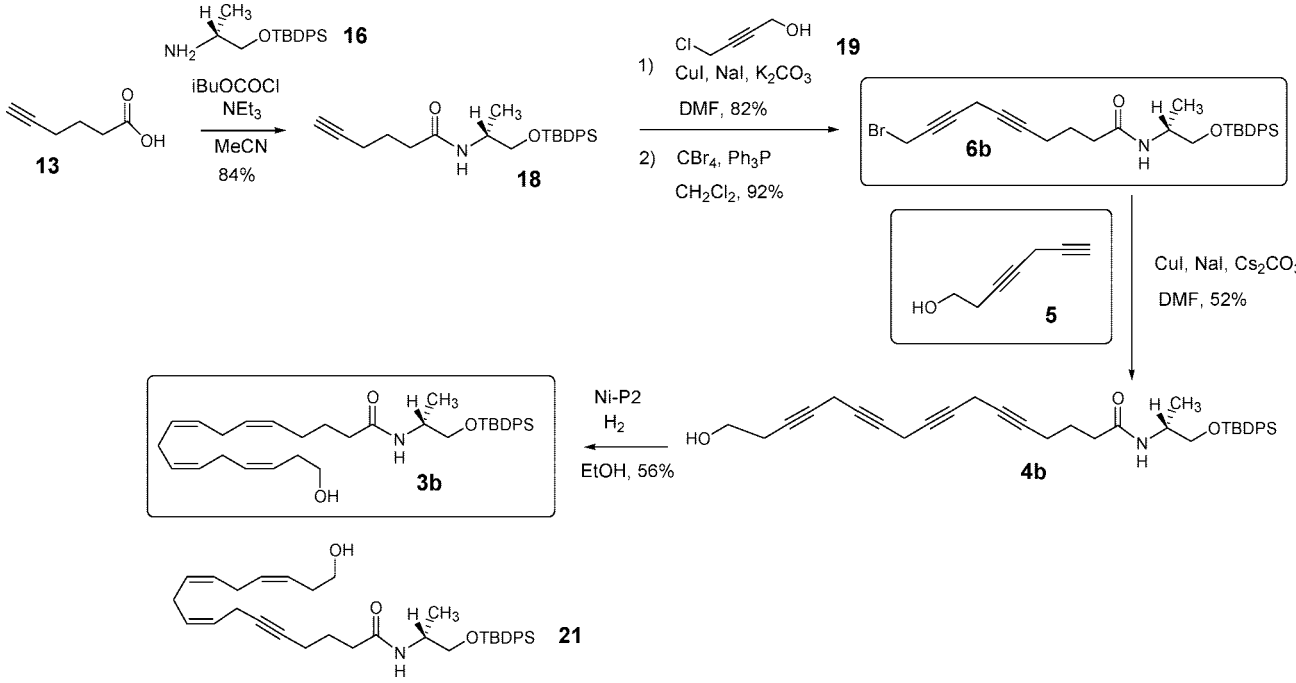

for the tetrayne ester **4a**, the tetrayneamide **4b** is highly unstable and was subsequently hydrogenated to its corresponding tetraene **3b** using Ni-P2 catalyst. The rate of hydrogenation of each alkyne functionality is not the same, with that closest to the carbonyl group being less reactive. Consequently, depending on the conditions (extent of nickel catalyst poisoning and reaction time), the reaction led to a mixture of the desired tetraene **3b**, partially reduced alkenes, together with the trieneyne intermediate **21**. Conditions[41] were optimized in order to obtain pure tetraene **3b**. This optimization was important, since separation of **3b** and **21** was difficult because of their similar chromatographic mobilities. Unfortunately, we could not increase the yield, which remained moderate (40% to 56%) mainly because of the instability of the starting tetrayne structure **4b**.

Pathway C. The synthetic pathways A and B described above are based on the synthesis of a tetrayne backbone **4**. However, these tetrayne intermediates **4** were highly unstable and difficult to work with. Therefore, a strategy encompassing a partially reduced alkyne−alkene backbone **7** was developed in order to confer stability to the precursors prior to the hydrogenation steps (Scheme 1).

Synthesis of the yne−ene−yne derivative **7** via a one-pot linchpin approach using 1,4-dichoro-2-*cis*-butene **22** was appealing. However, no information was found in the literature with regard to monoselectivity of the copper-mediated cross-coupling reaction between terminal alkynes and 1,4-dichoro-2-*cis*-butene **22** using the standard coupling conditions (NaI, CuI, base, DMF). A pilot experiment was undertaken using methyl 5-hexynoate[37] **23** and 3-butyne-1-ol **9** in place of the actual desired reactants **18** and **5**, respectively. The reaction was carried out with a stoichiometric amount of alkynes. In addition, a reaction was run with 2.0 equiv of terminal alkyne **23** in order to obtain a sample of the double substitution product for comparison in TLC and NMR analyses. However, in both cases, dichorobutene **22** had exhibited unexpected reactivity at the olefin carbon rather than the methylene chloride group, affording the chloride **24** as main product (81% yield, Scheme 5). It must be noted that this reaction was highly regioselective, with only one regioisomer (compound **24a**) formed. Unfortunately, as this was not the desired regioisomer **24b**, it was felt that no more progress could be made using this organometallic reaction.

Scheme 5. Regioselectivity of the Reaction of 1,4-*cis*-Dichlorobutene **22** with Terminal Alkyne **23**

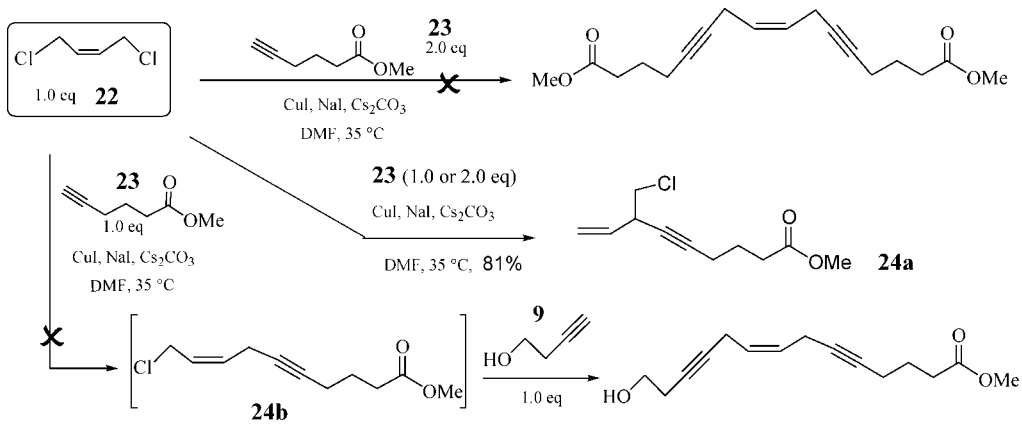

Scheme 6. Obtention of the Diamide **25**

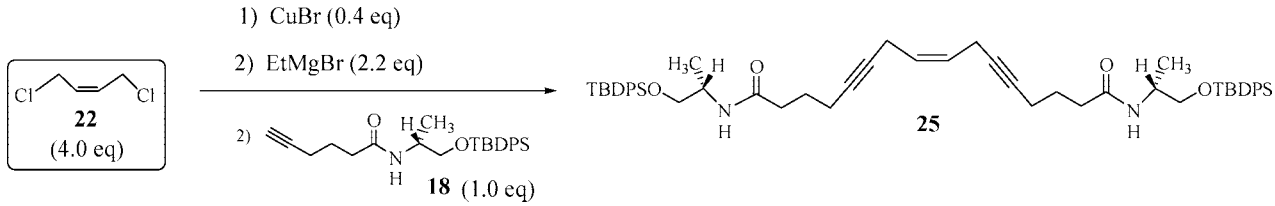

Scheme 7. Undesired Regioselectivity of the Cross-Coupling Reaction

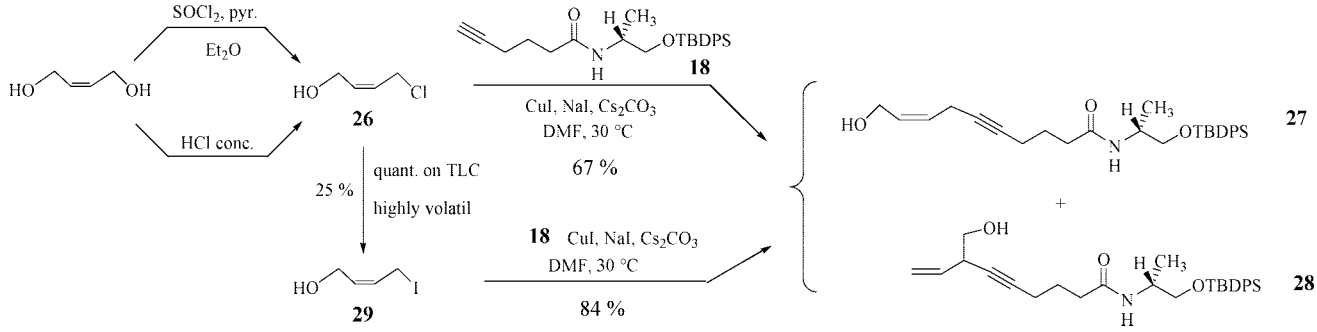

Alternative coupling reactions with dichloride **22** were then investigated under Taber coupling conditions. Using organomagnesium reagents with copper salts as catalysts, Taber was able to achieve[42] monoselectivity, good yields, and high regioselectivity in favor of a desired linear yne−ene−CH_2Cl substructure by carrying out the reaction at a temperature of 55 °C. As our alkyne precursor **18** is a secondary amide, an amount of 2 equiv of EtMgBr was added in order to counteract the reactivity of the amide structure. However, the amide function dramatically suffered from these organomagnesium conditions. In addition, both regioisomers were obtained as a 1:1 mixture (10%), the main isolated product being a symmetric disubstituted *cis*-butene **25** (Scheme 6, 27%).

Subsequently, a strategy based on the precursor 4-chloro-*cis*-buten-1-ol[43] **26** was examined. Unfortunately, poor regioselectivity was again observed, leading to an inseparable 1:1 mixture of both regioisomers **27** and **28** (Scheme 7).

In view of these coupling difficulties, we considered the possibility that the reactivity at the olefin carbon could be significantly decreased by substituting the methylene chloride with a more electrophilic iodine atom, so the reaction could be more directed. This conversion was undertaken following the Finkelstein reaction (yield not optimized). The resulting 4-iodo-*cis*-buten-1-ol **29** was then coupled to the alkyne **18** under the previous standard conditions. The ratio of the two regioisomers **27** and **28** was greatly improved, i.e., a 4-fold greater production of the desired product **27**.

When we initiated our studies of pathway C, we were rather optimistic[44] because the literature suggested that copper cross-coupling reactions were not associated with any regioselectivity problems.[45,35] The poor yields they obtained could be explained on the basis of the predictable instability of the polyskipped backbone. On the other hand, these SN/SN′ regioselectivity problems have been encountered by some authors, using somewhat different copper reaction conditions.[46]

Since pathways A and B were successful, we did not persevere in our efforts to obtain the yne−ene−yne structure **7**.

Synthesis of Probes 35, 37, 39, and 41. As reported in our preliminary study,[34] introduction of an arylazide group at the terminal pentyl chain of methanandamide does not disturb the CB2 binding affinity while its CB1 binding is somewhat affected. There is no way to know how this structural change would affect the interaction with the putative anandamide receptor. Binding or activation of the receptor could be disturbed because of the bulkiness of the aromatic moiety. Accordingly, we elected to use neighboring photophore groups no larger (and preferably smaller) than the 2-azido-5-iodobenzoate group. In addition, we believe that introduction of polar functionalities

Scheme 8. Synthesis of Probes **35**, **37**, **39**, and **41** from the Key Tetraene **3b**

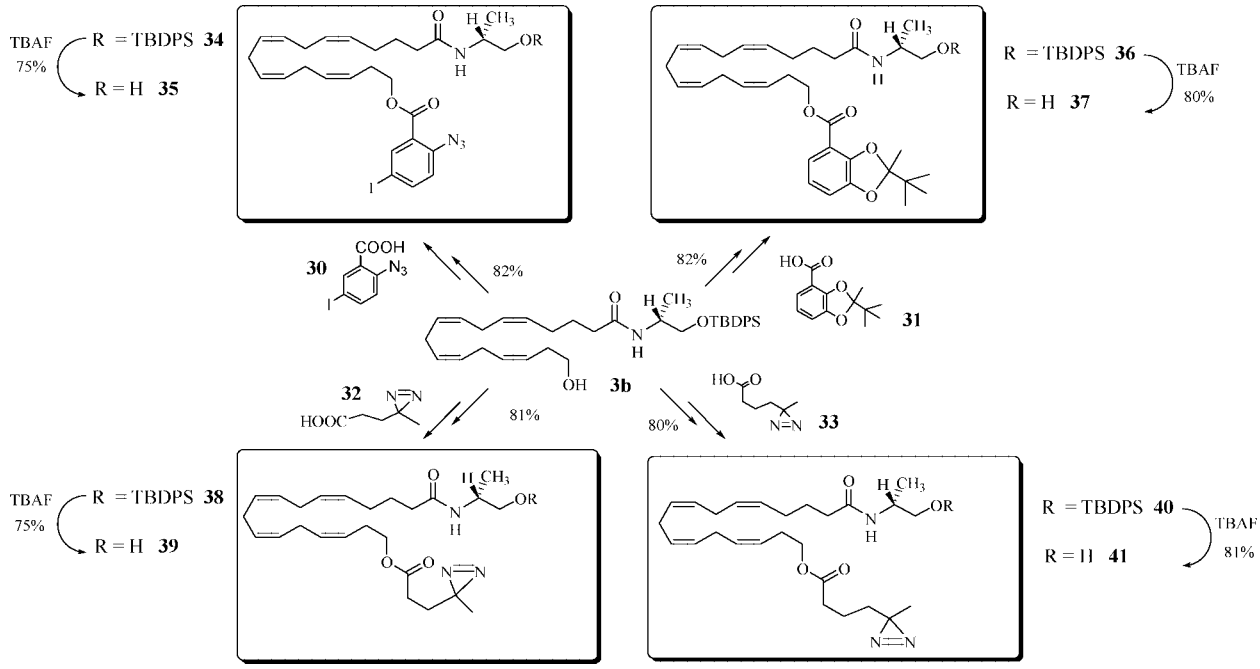

should be avoided, since the anandamide pentyl chain probably fits in a hydrophobic region of the receptor active site.

These two requirements drastically reduce the possibilities for the design of fluorescent probes, since most of the well-known fluorescent groups[47] (e.g., Alexa, BODIPY) are bulky and polar. We elected the 2-*tert*-butyl-2-methyl-1,3-benzodioxole-4-carboxylate (TBMB)[48] group. This particular structure, although not widely used for receptor−ligand studies, was attractive because of its relatively small size and reported fluorescence properties.

Concerning the design of novel photoactivatable probes, we turned our attention to short alkyl diazirins which are easier to handle than their alkyl azide homologues. Two chain lengths were tried, an approach expected to clarify SAR involving the tail chain binding region, at least for the CB1 and CB2 receptors.

Subsequently, a series of ester-linked probes were synthesized. Thus, Steglich esterification of the pivotal tetraene alcohol **3b** with photoreactive carboxylic acids such as 2-azido-5-iodobenzoic acid[49] **30**, TBMB carboxylic acid[48] **31**, and the C5 and C6 diazirin[50] precursors **32** and **33**, followed by fluoride cleavage of the silyl group, afforded the previously described probes **35** and then the three novel probes **37**, **39**, **41** respectively (Scheme 8).

As part of preliminary studies to optimize the photoirradiation conditions, UV spectra were recorded in methanol. Thus, upon irradiation at 254 nm, the arylazide function (at 265 nm) disappears within a few minutes (Figure 3). The diazirin absorption is weaker in comparison to the skipped bis-allylic system. The diazirin group was stable when irradiated at 254 nm (two shoulders at 348 and 367 nm, in agreement with literature data), regardless of the distance from the lamp. Furthermore, we found that upon irradiation of the diazirin **41** at 365 nm, the spectral scans obtained before, and various times after, were virtually superimposable over the entire UV range except in the diazirin absorption region (see expanded spectra in Figure 4).

Effect of Probes 35 and 37 on Angiogenesis. In our preliminary biological experiments,[34] the arylazide probe **35** was shown to bind the CB2 receptor while it poorly binds the CB1 receptor in comparison with anandamide. Replacement of the pentyl chain tail of anandamide with the fluorescent TBMB group (a slightly bulkier group than the arylazide group) resulted in the complete loss of CB1 and CB2 affinities. Effectively, probe **37** exhibited a K_i (μM) of 2.80 ± 0.05 and 1.02 ± 0.03 for CB1 and CB2 receptors, respectively (mean ± SE, N = 3).[51] Under the same conditions, anandamide shows a K_i (μM) of 0.07 ± 0.03 and 0.18 ± 0.02, respectively.

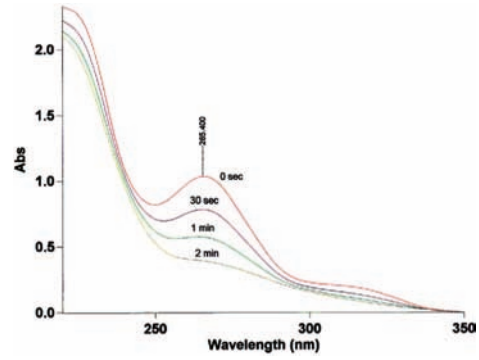

Figure 3. UV spectra of the arylazide **35** in methanol after 0, 30 s, 1 min, and 2 min of irradiation (lamp 254 nm, 15 W, d = 5 cm).

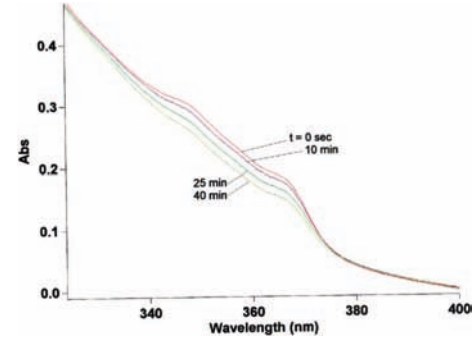

Figure 4. UV spectra of the diazirin **41** in methanol after 0, 10, 25, and 40 min of irradiation (lamp 365 nm, 6 W, d = 2.5 cm).

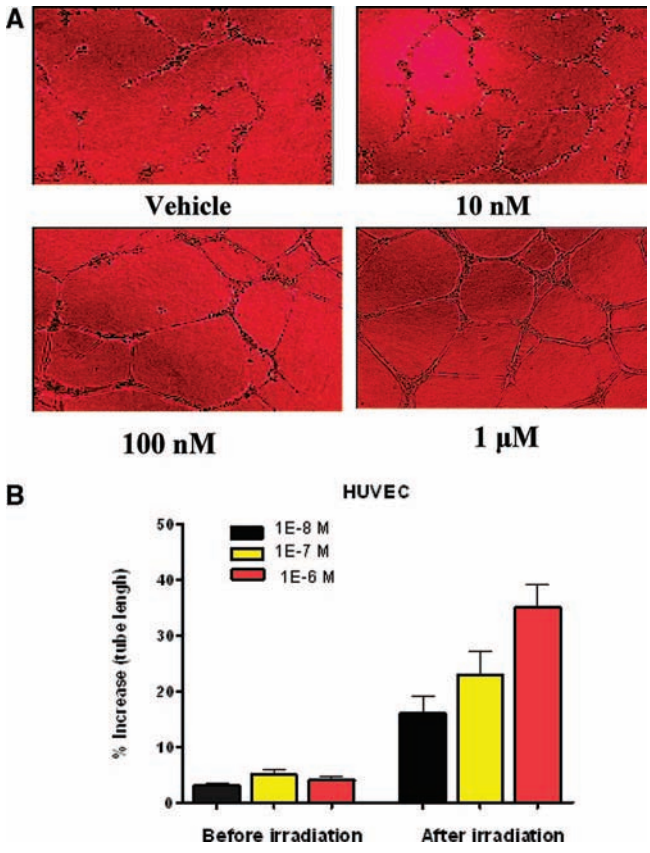

Figure 5. Effect of probe **35** on angiogenesis in HUVEC. (A) HUVEC cells were grown in 100 mm^2 plate up to 90% confluence and then harvested with versene (1× PBS−0.05% EDTA), and cell pellet was obtained by gentle centrifugation at 600*g* for 5 min. The cell pellet was resuspended in serum-free RPMI 1640 media and mixed with vehicle or probe **35** at the indicated final concentration. The cell mixture was then placed on Matrigel with or without UV irradiation as explained in Experimental Section and incubated at 37 °C for 36 h. The increase in cord length (tube formation) was assessed under microscope (10×), and images were captured as described in Experimental Section. The result shown here is a representative example of three similar results obtained from three separate experiments. (B) Quantitation of angiogenic response of probe **35** on HUVEC. After 36 h of incubation, the plates were fixed with Diff-Quick and images were captured using Nikon camera and analyzed using ImagePro software. Total length of the tubes formed by the endothelial cells in Matrigel was measured from three randomly chosen fields (10×) for each sample and analyzed by the ImagePro software (version 6.0) program. The results are analyzed as percent increase in cord length (tube formation) with respect to the corresponding vehicle-treated control. The results are expressed as the mean ± SEM of percent increase from three separate experiments.

As shown in Figure 5, probe **35** produces a dose-dependent increase in angiogenesis as evident by the increase in the length of tube formed by the human umbilical vein endothelial cells (HUVEC) in Matrigel. Interestingly, upon irradiation probe **35** produced a dramatic increase of the angiogenic response compared to the effect observed before irradiation (Figure 5B). This dose-dependent increase in the angiogenic response following irradiation strongly indicates that irradiation produced covalent binding of probe **35** to a specific site.

The involvement of "non-CB1/CB2 anandamide receptor" in probe **35**-induced angiogenesis was further confirmed from the results with CB1 receptor knockout HUVEC cells (CB1-KO HUVEC; Figure 6A shows that the CB1 receptor is reduced in the siRNA treated cells). Here again, probe **35** induced some nice tube length increases and irradiation dramatically stimulated the angiogenic response in tube formation assay (Figure 6B), producing strong dose-dependent increases (21%, 30%, 47% with 10 nM, 100 nM, and 1 μM, respectively, while they did not exceed 8% before irradiation). The degree of angiogenic response was statistically similar using CB1-KO HUVEC or HUVEC.

Studies from Kunos laboratories showed[28] that endothelial non-CB1/CB2 anandamide receptor-mediated vasorelaxation was inhibited by the selective non CB1/CB2 "anandamide receptor" antagonist O-1918. In the current study we found that probe **35**-induced increase in tube formation in CB1-KO HUVEC was significantly attenuated when cells were treated with probe **35** (after irradiation) in the presence of the anandamide receptor antagonist O-1918 (1 μM, Figure 6C). HUVEC does not express CB2 receptors (Mukhopadhyay et al., unpublished observations), and blockade of probe **35**-induced increase in angiogenic response in CB1-KO HUVEC by O-1918 strongly suggests that, in HUVEC, probe **35** produced angiogenesis by acting on "non-CB1/CB2 anandamide" receptors and these receptors are functionally active in HUVEC.

We tested the effect of probe **37** on HUVEC and CB1-KO HUVEC cells before and after irradiation under similar experimental conditions as probe **35**. First of all, as described for the probe **35**, the probe **37** also produced robust angiogenic response on HUVEC and CB1-KO HUVEC (Figure 7), showing statistically similar levels of response ($p > 0.05$). In addition, as expected because of its fluorescent properties (different from the photolabeling properties such as those of probe **35** or probe **41**), probe **37** did not exhibit any difference for angiogenic response before (data not shown) and after irradiation (Figure 7).

Effects of Probes 35 and 37 on MMP Activity. MMP (matrix metalloproteinase) plays an important role in the regulation of angiogenesis in relation to the degradation of the extracellular matrix so that endothelial cells can detach and migrate. Since probes **35** and **37** produce strong angiogenic responses in endothelial cells, we tested their effects on MMP (gelatinase; MMP2 and MMP9) activity. As shown in Figures 8 and 9, similar to the effect observed in tube formation assay, probes **35** and **37** produced dose-dependent increases in MMP activity in HUVEC and CB1-KO HUVEC. However, probe **37**-induced increase in MMP activity (Figure 9) was stronger compared to that produced by probe **35** (Figure 8). It is important to note that methanandamide produced relatively less increase in MMP activity (5%, 20%, and 28% increases with respect to vehicle-treated control at 10 nM, 100 nM, and 1 μM, respectively, in HUVEC; 10%, 25%, and 33% increases with respect to vehicle-treated control at 10 nM, 100 nM, and 1 μM, respectively, in CB1-KO HUVEC) compared to increase in MMP activity produced by probe **37**.

Further, as shown in Figure 10, in CB1-KO HUVEC cells probe **35**- and probe **37**-induced increases in MMP activity were significantly reduced by non-CB1/CB2 anandamide receptor antagonist O-1918. This suggests that probe **35** and probe **37** simulate MMP activity by acting on non-CB1/CB2 anandamide receptor.

MMP2 (also known as gelatinase A) is a constitutive enzyme that exists in pro- (72 kDa) and active (64 kDa) forms, and MMP9 is an inducible enzyme (92 kDa latent form). When secreted by cells, these enzymes act on their substrate in extracellular matrix proteins (gelatin for MMP2 and MMP9) to evoke cellular response. The secretion and activation mechanisms of MMPs are multistep processes and are mediated by the coordinated interactions of various factors including cell

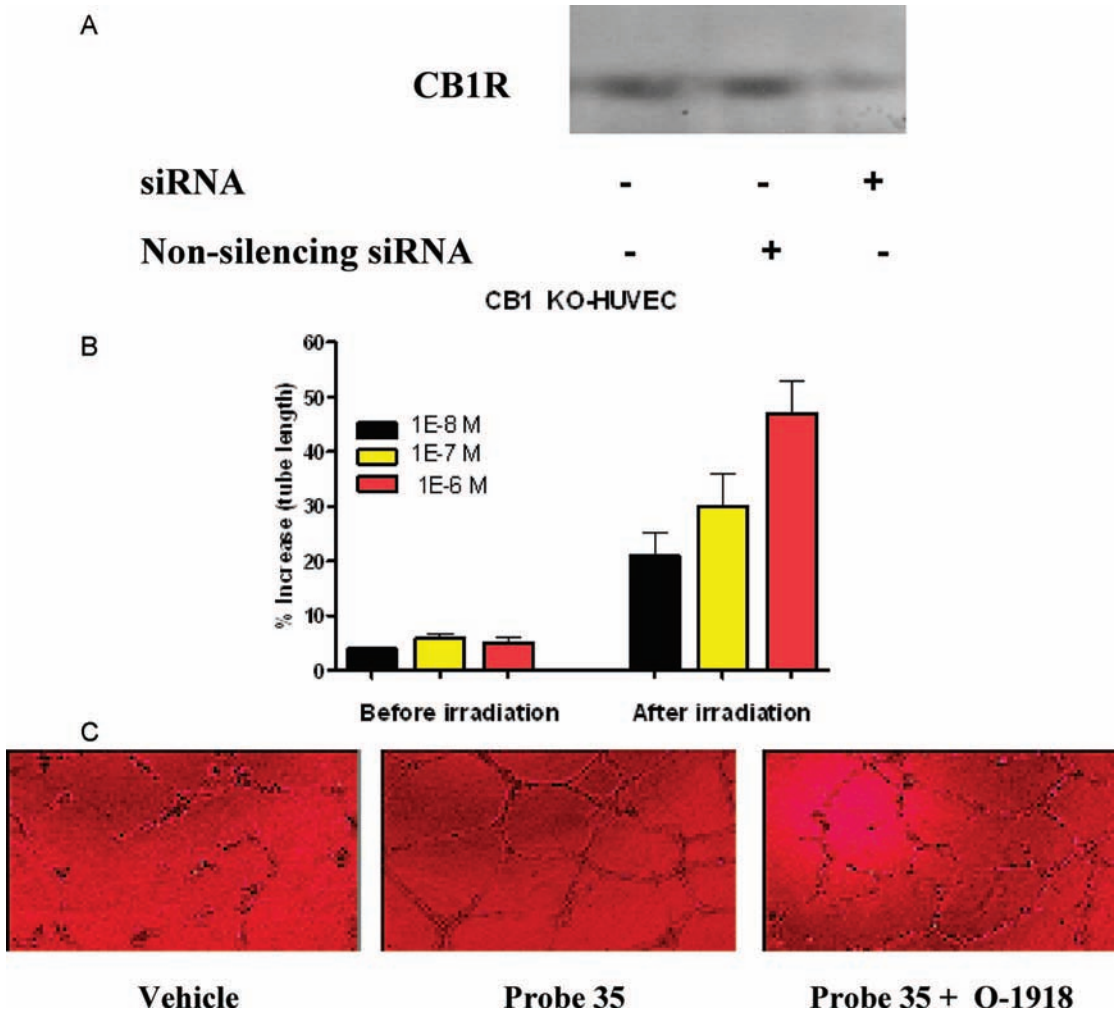

Figure 6. siRNA-mediated knocking down of CB1 receptor and effect of probe **35** on angiogenesis in CB1-KO HUVEC. (A) Western blot analysis of CB1 receptor expression in HUVEC and CB1-KO HUVEC. Cells were transfected with siRNA against CB1R or nonsilencing siRNA as described in Experimental Section. Thirty-six hours after transfection, cells were harvested and cell lysates were tested for CB1 receptor immunoreactivity as described in Experimental Section. (B) HUVEC and CB1-KO HUVEC were seeded in 100 mm^2 plates such that they grow to 90% confluence within 36 h after siRNA transfection and then harvested with versene (1× PBS−0.05% EDTA), and a cell pellet was obtained by gentle centrifugation at 600*g* for 5 min. The cell pellet was resuspended in serum-free RPMI 1640 media and mixed with vehicle or probe **35** at the indicated final concentration. The cell mixture was then placed on Matrigel with or without UV irradiation as explained in Experimental Section and incubated at 37 °C for 36 h. The formation of the tube was assessed under microscope, and images were captured and analyzed as described above. The results are expressed as the mean ± SEM percent increase in cord length (tube formation) with respect to the corresponding vehicle-treated control from three separate experiments. (C) Effect of anandamide receptor antagonist O-1918 on probe **35**-induced angiogenesis. CB1-KO HUVEC cells were treated with probe **35** (1 μM) in the presence and absence of O-1918 (1 μM). The extent of the tube formation was assessed as described above. Results are representative of three separate experiments with similar results.

surface MT1-MMP and tissue inhibitors of metalloproteases (TIMP 2 for MMP2 and TIMP1 for MMP9) with latent forms of MMPs (MMP2 and MMP9). Since probes **35** and **37** increased MMP activities, it is expected that activation of non-CB1/CB2 anandamide receptors evokes signal transduction that regulates TIMP−MMP interaction. We are currently testing the effect of probe **35** and probe **37** on TIMP−MMP interaction in endothelial cells. Since MMPs (MMP2 and MMP9) acting on extracellular matrix proteins produce cell detachment and evoke cell motility, we have also tested the effect of probes **35** and **37** on HUVEC cell motility. In cell migration assay probe **35** (following irradiation) produced dose-dependent 18%, 35%, and 54% increases with 10 nM, 100 nM, and 1 μM, respectively. Under similar assay conditions, probe **37** produced a relatively higher degree of increase in cell migration (27%, 40%, and 55% increases in cell migration with 10 nM, 100 nM, and 1 μM, respectively). Since increase in cell motility is an integral component of the angiogenesis process, the ability of the compounds to stimulate the cell migration strongly suggests that probes **35** and **37** bear strong positive angiogenic properties in endothelial cells.

In conclusion, we have accomplished a new convergent total synthesis of an arachidonic carbon skeleton using copper-mediated cross-coupling reactions between terminal alkynes and propargylic halides and using selective hydrogenation of skipped tetraynes **4**. Several synthetic routes were investigated to reach the pivotal tetraene **3b**. The latter compound was successfully transformed into four novel anandamide probes containing an arylazide, a diazirin, or a fluorescent group. We plan to extend this work by applying the same strategy to the preparation of other probes **2** with different eCB and elmiric acid head groups. These tools may be expected to advance significantly our understanding of the molecular events underlying receptor activation and signal transduction in the eCB system. The ability of probes **35** and **37** (a) to dose-dependently increase capillary-like tube formation in endothelial Matrigel assay in CB1-KO

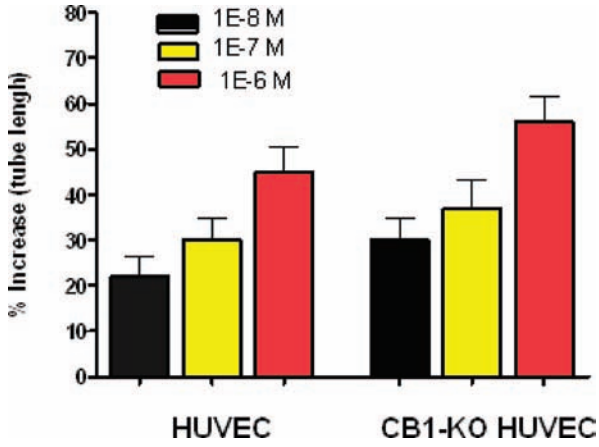

Figure 7. Effects of probe **37** on angiogenesis in HUVEC and CB1-KO HUVEC. The cells were grown in 100 mm^2 plates to 90% confluence and then harvested with versene (1× PBS−0.05% EDTA), and a cell pellet was obtained by gentle centrifugation at 600*g* for 5 min. The cell pellet was resuspended in serum-free RPMI 1640 media and mixed with vehicle or probe **37** at the indicated final concentration. The cell mixture was then placed on Matrigel as explained in Experimental Section and incubated at 37 °C for 36 h. The formation of the tube was assessed under microscope, and images were captured and analyzed as described above.

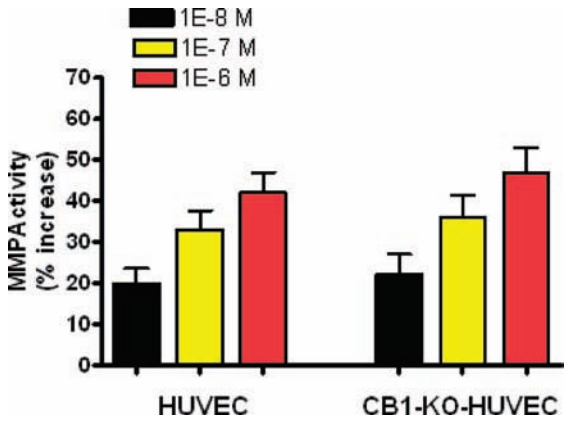

Figure 8. Effect of probe **35** on MMP activity. HUVEC or CB1-KO HUVEC cells were grown in six-well plates to 90% confluence and treated with vehicle or probe **35** at the indicated final concentration. The cells were either directly placed in an incubator at 37 °C or irradiated with UV (as described in the Experimental Section) and then placed in an incubator at 37 °C for 24 h. The MMP activity was measured from conditioned media as described in the Experimental Section. The results are analyzed as percent increase in enzyme activity with respect to corresponding vehicle treatment (basal activity) in the same cell line. The results are expressed as the mean ± SEM of percent increase from three separate experiments.

HUVEC in an O-1918-sensitive manner, (b) to stimulate MMP activity, and (c) to evoke an increase in cell migration strongly indicate that these compounds are acting as an agonist on non-CB1/CB2 anandamide receptors and the activation of the receptor functionally coupled to angiogenic response in endothelial cells. We will use a modified fluorescent probe (probe **37**) to develop a pharmacological ligand-binding assay as well as to localize the non-CB1/CB2 anandamide receptor in endothelial cells.

Experimental Section

Tetraeneamide 3b. Method A. Dimethoxytrityl ether 17 (50.07 mg, 57.19 mmol) was dissolved in 1,1,1,3,3,3-hexafluoro-2-propanol (HFIP, 500 μL, 100 mg/mL) and stirred overnight at 19 °C. A

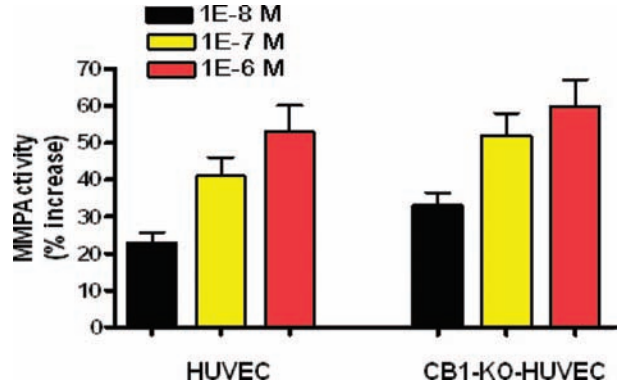

Figure 9. Effect of probe **37** on MMP activity. HUVEC or CB1-KO HUVEC cells were grown in six-well plates to 90% confluence and treated with vehicle or probe **37** at the indicated final concentration. The cells were either directly placed in an incubator at 37 °C or irradiated with UV (as described in the Experimental Section) and then placed in incubator for 24 h. The MMP activity was measured from conditioned media as described in the Experimental Section. The results are analyzed as percent increase in enzyme activity with respect to the corresponding vehicle treatment (basal activity) in the same cell line. The results are expressed as the mean ± SEM of percent increase from three separate experiments.

bright-orange color appears quickly, characteristic of the dimethoxytrityl carbocation release. The completion of the reaction was monitored by TLC (cyclohexane/AcOEt, 6/4, R_f = 0.45). The reaction was quenched by adding methanol (500 μL, discoloration) at room temperature. The solvents were removed under reduced pressure (without heating). The orange residue was dissolved in cyclohexane/ethyl acetate, 80/20) and plugged through a pad of Florisil to afford the deprotected homoallylic alcohol **3b** in 65% yield from acid **15**.

Method B. Nickel(II) acetate tetrahydrate (293.62 mg, 1.18 mmol, 0.64 equiv) was placed in a 50 mL two-necked round-bottom flask. Ethanol (16 mL) was added before the flask was placed under vacuum and then hydrogen to ensure no oxygen was present. A 1 M solution of $NaBH_4$ in ethanol (2.48 mL, 2.48 mmol, 1.35 equiv) was added. The resulting black solution was evacuated 3 times and then maintained under hydrogen atmosphere for 20 min. Ethylenediamine (878 μL, 13.14 mmol, 7.14 equiv) was added quickly via syringe, and the reaction mixture was stirred to stabilize for 15 min. The flask was evacuated 3 times. The tetrayne **4b** (1.04 g, 1.84 mmol, 1.0 equiv) was dissolved in ethanol (1.6 mL) and added quickly to the reaction flask. The mixture was evacuated 3 times and then maintained under hydrogen atmosphere for 8.5 h at 13 °C. The reaction mixture was quenched by addition of wet Et_2O (20 mL), followed by NH_4Cl (a pinch) to poison the catalyst. The reaction mixture was filtered through Celite which was washed with Et_2O. The solvents were removed under reduced pressure, and the residue was partitioned between Et_2O (100 mL) and sequentially $NaHSO_4$ (0.1 M, 5 mL), saturated aqueous NH_4Cl solution (2 × 5 mL), and brine (2.5 mL). The aqueous phases were extracted 4 times (100 mL), and the resulting organic phases were dried over $MgSO_4$, filtered, and concentrated under reduced pressure. The orange residue was chromatographed over Florisil (cyclohexane/ethyl acetate:, 99/1 to 92/8) to give the expected tetraene **3b** (588.16 mg, 56%) as a colorless oil. R_f = 0.36 (cyclohexane/ethyl acetate, 6/4). IR (cm^{-1}): 3574−3159 (OH/NH), 3012 (C−H), 2931 (C−H), 2857 (C−H), 1647 (NC═O), 1548 (CH═CH), 1428 (CH═CH), 1112 (C−O). ^{1}H NMR (300 MHz, $CDCl_3$) δ 7.80−7.51 (m, 4H, H arom), 7.50−7.25 (m, 6H, H arom), 5.67 (d, J = 8.3 Hz, NH), 5.57−5.20 (m, 8H, CH olefin), 4.15−4.00 (m, 1H, CHN), 3.75−3.49 (m, 4H, CH_2O and CH_2OSi), 2.90−2.71 (m, 6H, CH_2 bis-allylic), 2.42−2.27 (m, 2H, CH_2 allyl), 2.20−1.95 (m, 4H, CH_2 and CH_2 allyl), 1.75−1.57 (m, 2H, CH_2), 1.17 (d, J = 6.7 Hz, 3H, CH_3), 1.06 (s, 9H, *t*-Bu). ^{13}C NMR (75 MHz, $CDCl_3$) δ 172.14 (NC═O), 135.52 (CH arom), 133.32 (Cquat arom), 133.16 (Cquat arom), 130.79 (CH olefin), 129.82 (CH arom), 129.10 (CH olefin), 128.86

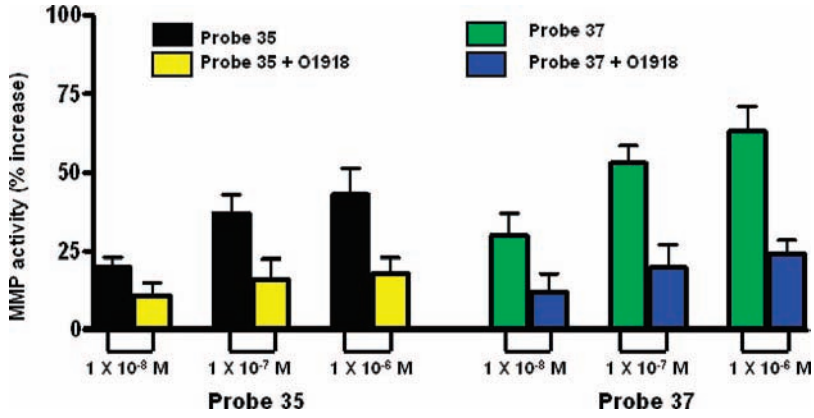

Figure 10. Effect of O-1918 on probe **35**- and probe **37**-induced MMP activity in CB1-KO HUVEC. CB1-KO HUVEC cells were grown in six-well plates to 90% confluence and treated with vehicle or probe **35** or probe **37** at the indicated final concentration in the presence and absence of O-1918 (1 μM). The cells were either directly placed in an incubator at 37 °C or irradiated with UV (as described in the Experimental Section) and then placed in an incubator for 24 h. The MMP activity was measured from conditioned media as described in the Experimental Section. The results are analyzed as percent increase in enzyme activity with respect to the corresponding vehicle treatment (basal activity) in the same cell line. The results are expressed as mean ± SEM of percent increase from three separate experiments.

(CH olefin), 128.68 (CH olefin), 128.22 (CH olefin), 128.00 (CH olefin), 127.76 (2 × CH olefin and CH arom), 125.73 (CH olefin), 66.83 (CH_2OH), 62.09 (CH_2OSi), 46.29 (CHN), 36.23 (CH_2), 30.90 (CH_2 allyl), 26.75 (*t*-Bu), 26.70 (CH_2 allyl), 25.76 (CH_2 bis-allyl), 25.65 (CH_2 bis-allyl), 25.55 (CH_2), 19.32 (Cquat *t*-Bu), 17.56 (CH3). MS (electrospray, positive mode): 596.5 (M + Na). Anal. Calcd for $C_{36}H_{51}NO_3Si$: C, 75.34; H, 8.96. Found: C, 75.42; H, 9.06.

Tetrayneamide 4b. The reaction flask was protected from light with aluminum foil, and workup procedure was run under dim light. A mixture of anhydrous Cs_2CO_3 (1.77 g, 5.43 mmol, 1.0 equiv), CuI (1.034 g, 5.43 mmol, 1.0 equiv), NaI (1.63 g, 10.86 mmol, 2.0 equiv), terminal diyne **5** (644.12 mg, 5.97 mmol, 1.1 equiv), and bromide **6b** (2.92 g, 5.43 mmol, 1.0 equiv) in DMF (11 mL) was stirred overnight at 40 °C. Upon cooling to 0 °C, the mixture was diluted with isopropyl ether (40 mL) and quenched with saturated NH_4Cl (6 mL). The two layers were separated, and the etheral layer was washed with brine (6 mL), followed by a 10% aqueous $Na_2S_2O_3$ solution (6 mL) and water (2 × 6 mL). The combined aqueous phases were re-extracted thrice with a mixture isopropyl ether/ether (1v/1v, 150 mL), dried over $MgSO_4$, and filtered. The solvents were removed in vacuo, avoiding heating and light. The residue was purified by flash chromatography on a pad of Florisil (cyclohexane/ethyl acetate, 95/5 to 70/30) to give 1.59 g (52%) of the expected tetrayne **4b** as a yellow oil (which darkened quickly on storage). Attempts to further purify it resulted in partial decomposition. Hence, it was used as such in the subsequent reaction as soon as possible. R_f = 0.48 (cyclohexane/ethyl acetate, 4/6). IR (cm^{-1}): 3432−3100 (OH, NH), 3071 (C−H), 2931 (C−H), 2858 (C−H), 2244 (C≡C), 2207 (C≡C), 1644 (NC═O), 1543 (CH═CH), 1471 (CH═CH), 1462 (CH═CH), 1427 (CH═CH), 1362 (CH═CH), 1318 (CH═CH), 1262 (C−O), 1110 (C−O), 1044 (C−O), 998. ^{1}H NMR (300 MHz, $CDCl_3$) δ 7.75−7.51 (m, 4H, H arom), 7.50−7.25 (m, 6H, H arom) 5.65 (br d, J = 8.1 Hz, 1H, NH), 4.17−4.00 (m, 1H, CHN), 3.75−3.50 (m, 3H, CHOSi and CH_2O), 3.58 (dd, J = 3.9 Hz, J = 10.1 Hz, 1H, CHOSi), 3.25−3.00 (m, 6H, CH_2 bis-propargylic), 2.57−2.31 (m, 2H, CH_2 propargylic), 2.31−2.05 (m, 4H, CH_2 and CH_2 propargylic), 1.85−1.65 (m, 2H, CH_2), 1.16 (d, J = 6.7 Hz, 3H, CH_3), 1.05 (s, 9H, *t*-Bu). ^{13}C NMR (75 MHz, $CDCl_3$) δ 171.64 (NC═O), 135.50 (CH arom), 133.29 (Cquat arom), 133.15 (Cquat arom), 129.82 (CH arom), 127.76 (CH arom), 79.73 (C≡C), 77.31 (C≡C), 75.87 (C≡C), 75.06 (C≡C), 74.77 (C≡C), 74.65 (C≡C), 74.35 (C≡C), 74.14 (C≡C), 66.78 (CH_2OSi), 61.00 (CH_2OH), 46.36 (CHN), 35.47 (CH_2), 26.86 (*t*-Bu), 24.49 (CH_2), 23.02 (CH_2 propargylic), 19.31 (Cquat *t*-Bu), 18.14 (CH_2 propargylic), 17.52 (CH_3), 9.73 (CH_2 bis-propargylic). MS (electrospray, positive mode): 566.4 (M + H), 588.6 (M + Na).

General Procedure for the Deprotection of the TBDPS Group. TBAF (1.5 equiv, 1 M in THF) was added dropwise to a solution of silylated ether **34**, **36**, **38**, or **40** (1.0 equiv) in anhydrous THF (10 mL/mmol) at 0 °C. The reaction mixture was directly plugged through a pad of Florisil using cyclohexane/CH_2Cl_2, 1/1, then CH_2Cl_2, then increasing concentration of methanol in cyclohexane to provide the corresponding pure alcohol.

Fluorescent Probe 37. White powder. 80% yield. R_f = 0.57 (CH_2CH_2/MeOH, 96/4). IR (cm^{-1}): 3719−3101 (OH/NH), 2952 (C−H), 2931 (C−H), 2851 (C−H), 1709 (COOR), 1649 (NC═O), 1546 (CH═CH), 1468 (CH═CH), 1428 (CH═CH), 1376 (CH═CH), 1297 (C−O), 1250, 1234 (C−O), 1149 (C−O), 1113, 1068, 1051. ^{1}H NMR (500 MHz, $CDCl_3$) δ 7.29 (d, J = 7.9 Hz, 1H, H arom), 6.83 (d, J = 7.9 Hz, 1H, H arom), 6.74 (t, J = 7.9 Hz, 1H, H arom), 5.70 (br s, 1H, NH), 5.55−5.42 (m, 2H, H olefin), 5.42−5.26 (m, 6H, H olefin), 4.39−4.18 (m, 2H, CH_2O), 4.14−3.95 (m, 1H, CHN), 3.64 (dd, J = 10.9 Hz and J = 3.2 Hz, 1H, CHOSi), 3.51 (dd, J = 10.9 Hz and J = 6.1 Hz, 1H, CHOSi), 3.02−2.66 (m, 6H, CH_2 bis-allyl), 2.58−2.42 (m, 2H, CH_2 allyl), 2.25−2.13 (m, 2H, CH_2), 2.12−1.94 (m, 2H, CH_2 allyl), 1.80−1.64 (m, 2H, CH_2), 1.58 (s, 3H, CH3), 1.14 (d, J = 6.8 Hz, 3H, CH3), 1.06 (s, 9H, *t*-Bu). ^{13}C NMR (75 MHz, $CDCl_3$) δ 173.67 (NC═O), 164.84 (COOR), 149.37 (Cquat arom), 148.81 (Cquat arom), 130.42 (CH olefin), 129.11 (CH olefin), 128.75 (CH olefin), 128.29 (CH olefin), 128.07 (CH olefin), 127.98 (CH olefin), 127.70 (CH olefin), 125.26 (CH olefin), 124.69 (Cquat), 121.74 (CH arom), 120.15 (CH arom), 112.1 (Cquat), 111.32 (CH arom), 67.42 (CH_2OH), 64.12 (CH_2O), 47.84 (CHN), 39.56 (Cquat), 36.08 (CH_2), 26.93 (CH_2 allyl), 26.65 (CH_2 allyl), 25.75 (CH_2 bis-allyl), 25.65 (CH_2 bis-allyl), 25.48 (CH_2), 24.46 (*t*-Bu), 20.26 (CH_3), 17.04 (CH_3). MS (electrospray, positive mode): 576.20 (M + Na), 1130.53 (M × 2 + Na). Anal. Calcd for $C_{33}H_{47}NO_6$: C, 71.58; H, 8.56. Found: C, 71.63; H, 8.42.

Diazirin Probe 39. Colorless oil. 75% yield. R_f = 0.38 (CH_2Cl_2/MeOH: 96/4). IR (cm^{-1}): 3602−3137 (OH/NH), 3012 (C−H), 2930 (C−H), 2862 (C−H), 1736 (COOR), 1643 (NC═O), 1545 (CH═CH), 1450 (CH═CH), 1386 (CH═CH), 1252 (C−O), 1177 (C−O), 1051. ^{1}H NMR (400 MHz, $CDCl_3$) δ 5.61 (br s, 1H, NH), 5.52−5.41 (m, 1H, H olefin), 5.41−5.26 (m, 7H, H olefin), 4.14−3.99 (m, 3H, CHN and CH_2OC), 3.64 (dd, J = 3.4 Hz and J = 10.9 Hz, 1H, CHO), 3.51 (dd, J = 6.1 Hz and J = 10.9 Hz, 1H, CHO), 2.87−2.71 (m, 6H, CH_2 bis-allyl), 2.45−2.33 (m, 2H, CH_2 allyl), 2.17 (t, J = 7.7 Hz, 2H, CH_2), 2.15 (t, J = 7.8 Hz, 2H, CH_2), 2.13−2.06 (m, 2H, CH_2 allyl), 1.75−1.64 (m, 4H, CH_2), 1.60 (br s, 1H, OH), 1.15 (d, J = 6.8 Hz, 3H, CH3), 1.00 (s, 3H, CH3). ^{13}C NMR (100 MHz, $CDCl_3$) δ 173.54 (NC═O), 172.32 (COOR), 130.75 (CH olefin), 129.12 (CH olefin), 128.76 (CH olefin), 128.36 (CH olefin), 128.30 (CH olefin), 128.05 (CH olefin), 127.88 (CH olefin), 124.81 (CH olefin), 67.39 (CH_2OH), 64.07 (CH_2O), 47.82

(CHN), 36.07 (CH_2), 29.68 (CH_2), 28.76 (CH_2), 26.82 (CH_2 allyl), 26.64 (CH_2 allyl), 25.65 (CH_2 bis-allyl), 25.48 (CH_2), 24.89 (Cquat diazirin), 19.66 (CH3), 17.04 (CH3). MS (electrospray, positive mode): 468.13 (M + Na), 440.20 (M − N_2 + Na). Anal. Calcd for $C_{25}H_{39}N_3O_4$: C, 67.39; H, 8.82. Found: C, 67.15; H, 8.97.

Diazirin Probe 41. Pale-yellow oil. 81% yield. R_f = 0.51 (CH_2Cl_2/MeOH, 96/4). IR (cm^{-1}): 3669−3109 (OH/NH), 3012 (C−H), 2931 (C−H), 2857 (C−H), 1734 (COOR), 1643 (NC═O), 1545 (CH═CH), 1453 (CH═CH), 1386 (CH═CH), 1256 (C−O), 1173 (C−O), 1051, 994. ^{1}H NMR (300 MHz, $CDCl_3$) δ 5.66 (br s, 1H, NH), 5.55−5.41 (m, 1H, H olefin), 5.41−5.23 (m, 7H, H olefin), 4.17−3.97 (m, 3H, CHN and CH_2O), 2.88 (t, J = 5.5 Hz, 1H, OH), 2.85−2.67 (m, 6H, CH_2 bis-allyl), 2.49−2.32 (m, 2H, CH_2 allyl), 2.26- (t, J = 7.3 Hz, 2H, CH_2), 2.17 (t, J = 7.6 Hz, 2H, CH_2), 2.12−1.94 (m, 2H, CH_2 allyl), 1.80−1.61 (m, 2H, CH_2), 1.57−1.43 (m, 2H, CH_2), 1.42−1.26 (m, 2H, CH_2), 1.14 (d, J = 6.8 Hz, 3H, CH3), 0.98 (s, 3H, CH3). ^{13}C NMR (75 MHz, $CDCl_3$) δ 173.61 (NC═O), 173.02 (COOR), 130.70 (CH olefin), 129.10 (CH olefin), 128.74 (CH olefin), 128.34 (CH olefin), 128.29 (CH olefin), 128.04 (CH olefin), 127.89 (CH olefin), 124.87 (CH olefin), 67.29 (CH_2OH), 63.80 (CH_2O), 47.77 (CHN), 36.06 (CH_2), 33.69 (CH_2), 33.51 (CH_2), 26.85 (CH_2 allyl), 26.63 (CH_2 allyl), 25.63 (br, CH_2 bis-allyl), 25.47 (Cquat diazirin), 19.68 (CH3), 19.46 (CH_2), 17.03 (CH3). MS (electrospray, positive mode): 482.1 (M + Na), 454.2 (M − N_2 + Na). Anal. Calcd for $C_{26}H_{41}N_3O_4$: C, 67.94; H, 8.99. Found: C, 68.09; H, 9.12.

siRNA and Transfection. Several siRNA against the CB1 cannabinoid receptors were constructed and synthesized by Ambion (Austin, TX) using proprietary methods. The specificity of the siRNA sequence was checked via BLAST search. For silencing CB1 receptors, HUVEC cells were grown to 70% confluence. Thereafter, cells were transfected with CB1 cannabinoid receptor-specific silencing siRNA or nonsilencing siRNA using siPORT siRNA electroporation kit (Ambion, TX) following the manufacturer's instructions. In brief, a cell pellet (approximately 7 × 104) was collected, suspended in 75 μL of SiRNA electroporation buffer (Ambion) and mixed with 1.5 μg of siRNA or nonsilencing siRNA. The mixture was subjected to electroporation in an electroporation cuvette (1 mm pass) under conditions identified in optimizing experiments. Following electroporation, samples in the cuvette were incubated at 37 °C for 10 min and cells were transferred to a culture dish with prewarmed growth media. Cells were incubated at 37 °C in a 95% O_2/5% CO_2 incubator until they were analyzed.

In Vitro Angiogenesis Assay (Tube Formation Assay). The tube formation assay was performed as described previously.[52] Briefly, 24-well plates were coated with 300 μL of 1:1 mixture of RPMI 1640 and Matrigel (10 mg/mL, Invitrogen) and incubated at 37 °C for 1 h to promote gelling. HUVECs (40 000) in 0.5 mL of serum-free RPMI 1640 medium with varying concentrations of drug were added to each well. For a positive control, bFGF was added at a concentration of 5 ng/mL. All test samples were performed in triplicate. After 36 h of incubation, the plates were fixed with Diff-Quick and images were captured using a Nikon camera and analyzed using ImagePro software. The total length of the tubes formed by the endothelial cells was measured from three randomly chosen fields (10×) for each sample and analyzed by the ImagePro software program. This experiment was performed in triplicate for each sample three times.

Irradiation of Ligands. The endothelial cells were grown in six-well plates at 90% confluence and then placed in a C-65 cabinet attached with one 8-W EL lamp [UVLMS-38 8-W UV lamp (14.8 in. length × 3.8 in. width × 2.5 in. depth) equipped with low, medium, and long range (365/302/254 nm) UV-generating wavelength 365/302/254 nm; UVP, Upland, CA]. The cells were treated with test drugs and irradiated for 1−15 min at 280−315 nm range. The distance between the light source and the cells was 10 in. The cell viability was assessed before and after irradiation, and no significant difference in cell viability was observed up to 10 min of exposure. Therefore, the experiment described herein was performed after 5 min of excitation.

Measurement of MMP Activity. The MMP (matrix metalloproteinase) activity was measured using Enzchek gelatinase/collagenase assay kit (Molecular Probes) following the manufacturer's protocol using a multiwell microplate reader. The cells were plated in a six-well plate and at 90% confluence treated with vehicle or test drugs for 24 h. Conditioned media samples (100 μL) were collected (following treatment) and added into the wells of a 96-well plate in triplicate followed by 80 μL of 1× reaction buffer (from Molecular Probes kit) in each assay well. Then 20 μL of "DQ gelatin" (6 μg/mL, Molecular Probes) was added to each well and the mixture was incubated in the plate for 24 h at 37 °C in the dark. After the incubation period, fluorescence is measured using a microplate reader (Victor S23-271-05) at excitation/emission of 485/530 nm. A standard curve is simultaneously developed incubating the same amount of substrate "DQ gelatin" (6 μg/mL) with varying amounts (0.01−0.04 μg/mL) of purified Clostridium collagenase enzyme (Molecular Probe kit). The digestion of the substrate with the enzyme will remove the quenching of heavily loaded fluorescence labeling in gelation, and the increase in the fluorescence reading is directly proportional to the enzyme activity. The experiment is performed in triplicate, and data are analyzed using GraphPad Prism software. For experiments with probe **37**, background fluorescence reading was subtracted from the experimental readings. The background fluorescence of probe **37** was obtained by adding probe **37** at different concentrations (as used to treat the cells) into complete media and then measuring fluorescence after 24 h as described above.

Cell Migration Assay. The cell migration assay was performed as described previously[53] in a 48-well microchemotaxis chamber (Neuro Probe, Inc., MD). Briefly, polyester membranes with 10 μm pores (Neuro Probe, Inc., MD.) were coated with a 0.1 mg/mL of collagen IV (Invitrogen) in doubly distilled water and then dried for 1 h. HUVECs and CB1-KO HUVEC were harvested using Versene (Sigma; St Louis, MO) and resuspended in RPMI 1640 containing 0.1% BSA. The bottom chamber was loaded with 30 000 cells, and the filter was laid over the cells. The microchamber was then inverted and incubated at 37 °C for 2 h. After reinversion of the chamber to its upright position, the upper wells were then loaded with RPMI 1640 containing 0.1% BSA and test drugs. bFGF was added at a concentration of 5 ng/mL as a positive control. The chamber was then reincubated at 37 °C for 6 h, and the filters were fixed and stained using Diff-Quick (Baxter Healthcare Corp., IL). The cells that migrated through the filter were quantitated by counting the center of each well at ×20 using an Olympus CK 40 microscope. Each condition was studied in triplicate wells, and each experiment was performed three times.

Acknowledgment. We gratefully acknowledge Pr. Joseph Vercauteren (Laboratory of Pharmacognosy, Montpellier, France) for allowing us to record ESI mass spectra in his laboratory. The authors are deeply grateful to Pr. Jean-Yves Lallemand and the ICSN for their generous financial support. We thank Dr. Eric G. Spokas (Rider University, Lawrenceville, NJ) for a critical reading of the manuscript. This work was supported by a NC Biotech grant to S.M., NIH Grant U24-DA 12385, and U.S. Army Medical Research and Material Command (Grant 07-1-0418).

Supporting Information Available: General methods and experimental procedures together with ^{1}H NMR and ^{13}C NMR data and spectra for every new compound. This material is available free of charge via the Internet at http://pubs.acs.org.

References

(1) Hanus, L. O. Discovery and isolation of anandamide and other endocannabinoids. *Chem. Biodiversity* **2007**, *4*, 1828–1841.

(2) Devane, W. A.; Hanus, L.; Breuer, A.; Pertwee, R. G.; Stevenson, L. A.; Griffin, G.; Gibson, D.; Mandelbaum, A.; Etinger, A.; Mechoulam, R. Isolation and structure of a brain constituent that binds to the cannabinoid receptor. *Science* **1992**, *258*, 1946–1949.

(3) (a) Burstein, S. H.; Adams, J. K.; Bradshaw, H. B.; Fraioli, C.; Rossetti, R. G.; Salmonsen, R. A.; Shaw, J. W.; Walker, J. M.; Zipkin, R. E.; Zurier, R. B. Potential anti-inflammatory actions of the elmiric (lipoamino) acids. *Bioorg. Med. Chem.* **2007**, *15*, 3345–3355. (b) Burstein, S. The elmiric acids: biologically active anandamide analogs. *Neuropharmacology* **2007**, doi:10.1016/j.neuropharm.2007.11.011.
(4) Kogan, N. M.; Mechoulam, R. J. The chemistry of endocannabinoids. *Endocrinol. Invest.* **2006**, *29*, 3–14.
(5) Milman, G.; Maor, Y.; Abu-Lafi, S.; Horowitz, M.; Gallily, R.; Batkai, S.; Mo, F. M.; Offertaler, L.; Pacher, P.; Kunos, G.; Mechoulam, R. *N*-Arachidonoyl L-serine, an endocannabinoid-like brain constituent with vasodilatory properties. *Proc. Natl. Acad. Sci. U.S.A.* **2006**, *103*, 2428–2433.
(6) Saghatelian, A.; McKinney, M. K.; Bandell, M.; Patapoutian, A.; Cravatt, B. F. A FAAH-regulated class of *N*-acyl taurines that activates TRP ion channels. *Biochemistry* **2006**, *45*, 9007–9015.
(7) Mechoulam, R. *Cannabinoids as Therapeutics*; Mechoulam, R., Ed.; Milestones in Drug Therapy; Birkhauser Publisher: Basel, Switzerland, 2005.
(8) Grimaldi, C.; Bibulco, M. Anandamide, an endogenous ligand of cannabinoids receptors, inhibits human breast cancer cell proliferation through a lipid rafts mediated mechanism. *Pharmacologyonline* **2007**, *1*, 1–45.
(9) Di Marzo, V.; Petrosino, S. Endocannabinoids and the regulation of their levels in health and disease. *Curr. Opin. Lipidol.* **2007**, *18*, 129–140.
(10) Howlett, A. C.; Barth, F.; Bonner, T. I.; Cabral, G.; Casellas, P.; Devane, W. A.; Felder, C. C.; Herkenham, M.; Mackie, K.; Martin, B. R.; Mechoulam, R.; Pertwee, R. G. International Union of Pharmacology. XXVII. Classification of cannabinoid receptors. *Pharmacol. Rev* **2002**, *54*, 161–202.
(11) (a) Steffens, M.; Zentner, J.; Honegger, J.; Feuerstein, T. J. Binding affinity and agonist activity of putative endogenous cannabinoids at the human neocortical CB1 receptor. *Biochem. Pharmacol.* **2005**, *69*, 169–178. (b) Porter, A. C.; Sauer, J. M.; Knierman, M. D.; Becker, G. W.; Berna, M. J.; Bao, J.; Nomikos, G. G.; Carter, P.; Bymaster, F. P.; Leese, A. B.; Felder, C. C. Characterization of a novel endocannabinoid, virodhamine, with antagonist activity at the CB1 receptor. *J. Pharmacol. Exp. Ther.* **2002**, *301*, 1020–1024.
(12) Fride, E.; Gobshtis, N. Endocannabinoids and their receptors: physiology, pathology and pharmacology. *Immunol., Endocr. Metab. Agents Med. Chem.* **2007**, *7*, 157–173.
(13) A full issue of the *British Journal of Pharmacology* (**2008**, *153* (2)) is dedicated to reviews and topics on the CB2 receptor, stemming from a meeting "CB2 Receptors: New Vistas" that was held in Canada in June 2007.
(14) (a) Liu, J.; Wang, L.; Harvey-White, J.; Huang, B. X.; Kim, H. Y.; Luquet, S.; Palmiter, R. D.; Krystal, G.; Rai, R.; Mahadevan, A.; Razdan, R. K.; Kunos, G. Multiple pathways involved in the biosynthesis of anandamide. *Neuropharmacology* **2008**, *54*, 1–7. (b) McPartland, J. M.; Norris, R. W.; Kilpatrick, C. W. Coevolution between cannabinoid receptors and endocannabinoid ligands. *Gene* **2007**, *397*, 126–135.
(15) Demuth, D. G.; Molleman, A. Cannabinoid signalling. *Life Sci.* **2006**, *78*, 549–563.
(16) Felder, C. C.; Dickason-Chesterfield, A. K.; Moore, S. A. Cannabinoids biology: the search for new therapeutic targets. *Mol. Interventions* **2006**, *6*, 149–161.
(17) Smita, K.; Sushil Kumar, V.; Premendran, J. S. Anandamide: an update. *Fundam. Clin. Pharmacol.* **2007**, *21*, 1–8.
(18) Alexander, S. P.; Kendall, D. A. The complications of promiscuity: endocannabinoid action and metabolism. *Br. J. Pharmacol.* **2007**, *152*, 602–623.
(19) Fowler, C. J. The contribution of cyclooxygenase-2 to endocannabinoid metabolism and action. *Br. J. Pharmacol.* **2007**, *152*, 594–601.
(20) Brown, A. J. Novel cannabinoid receptors. *Br. J. Pharmacol.* **2007**, *152*, 567–575.
(21) Di Marzo, V.; De Petrocellis, L. Non-CB1 Non CB2 Receptors for Endocannabinoids. In *Endocannabinoids: The Brain and Body's Marijuana and Beyond*; Onaivi, E. S., Sugiura, T., Di Marzo, V., Eds.; Taylor & Francis: Boca Raton, FL, 2006; Vol. 15, pp 1−174.
(22) Begg, M.; Pacher, P.; Batkai, S.; Osei-Hyiaman, D.; Offertaler, L.; Mo, F. M.; Liu, J.; Kunos, G. Evidence for novel cannabinoid receptors. *Pharmacol. Ther.* **2005**, *106*, 133–145.
(23) Pertwee, R. G. Novel pharmacological targets for cannabinoids. *Curr. Neuropharmacol.* **2004**, *2*, 9–29.
(24) Fride, E.; Foox, A.; Rosenberg, E.; Faigenboim, M.; Cohen, V.; Barda, L.; Blau, H.; Mechoulam, R. Milk intake and survival in newborn cannabinoid CB1 receptor knockout mice: evidence for a "CB3" receptor. *Eur. J. Pharmacol.* **2003**, *461*, 27–34.
(25) Di Marzo, V.; De Petrocellis, L.; Fezza, F.; Ligresti, A.; Bisogno, T. Anandamide receptors. *Prostaglandins, Leukotrienes Essent. Fatty Acids* **2002**, *66*, 377–391.
(26) Perry, S. N.; Johnson, I. J.; Mukhopadhyay, S. Anandamide Mediated Angiogenesis: Interplay between CB1 Receptor and Non CB1/CB2 Anandamide Receptor. *Proceedings of the 16th Annual Symposium of Cannabinoids*, Burlington, VT, 2006; International Cannabinoid Research Society, 2006; p 61.
(27) Hilderbrandt, S.; Johnson, I. J.; Mukhopadhyay, S. CB1 Receptor and Non-CB1/CB2 Annadmaide Receptor Mediated Differential S-Nitrosylation of MMP: A Novel Angiogenic Switch for the Regulation of Angiogenesis (2008). *Proceedings of the 18th Annual Symposium of Cannbinoids*, Burlington, VT, 2008; International Cannabinoid Research Society, 2008; p 17.
(28) McCollum, L.; Howlett; Mukhopadhyay, S. Anandamide-mediated CB1/CB2 cannabinoid receptor—independent nitric oxide production in rabbit aortic endothelial cells. *J. Pharmacol. Exp. Ther.* **2007**, *321*, 930–937.
(29) Daly, C. J.; McGrath, J. C. Fluorescent ligands, antibodies, and proteins for the study of receptors. *Pharmacol. Ther.* **2003**, *100*, 101–118.
(30) Vodovozova, E. L. Photoaffinity labeling and its application in structural biology. *Biochemistry (Moscow)* **2007**, *72*, 1–20.
(31) (a) Brase, S.; Gil, C.; Knepper, K.; Zimmermann, V. Organic azides: an exploding diversity of a unique class of compounds. *Angew. Chem., Int. Ed.* **2005**, *44*, 5188–240. (b) Bucher, G. Photochemical Reactivity of Azides. In *CRC Handbook of Organic Photochemistry and Photobiology*, 2nd ed.; Horspool, W. M., Lenci, F., Eds.; CRC Press: Boca Raton, FL, 2004; Chapter 44. (c) Blencowe, A.; Hayes, W. Development and application of diazirines in biological and synthetic macromolecular systems. *Soft Matter* **2005**, *1*, 178–205. (d) Sadakane, Y.; Hatanaka, Y. Photochemical fishing approaches for identifying target proteins and elucidating the structure of a ligand-binding region using carbene-generating photoreactive probes. *Anal. Sci.* **2006**, *22*, 209–218.
(32) (a) Abadji, V.; Lin, S.; Taha, G.; Griffin, G.; Stevenson, L. A.; Pertwee, R. G.; Makriyannis, A. (*R*)-Methanandamide: a chiral novel anandamide possessing higher potency and metabolic stability. *J. Med. Chem.* **1994**, *37*, 1889–1893. (b) Haller, V. L.; Cichewicz, D. L.; Welch, S. P. Non-cannabinoid CB1, non-cannabinoid CB2 antinociceptive effects of several novel compounds in the PPQ stretch test in mice. *Eur. J. Pharmacol.* **2006**, *546*, 60–68.
(33) It must be realized that we are not looking for a specific ligand for CB_1 or CB2 receptors but for a mimic of eCBs, mainly anandamide, to search for novel putative receptors. However, very little is known about these targeted new receptors. It is therefore rather difficult to anticipate what structural requirements would be needed for a synthetic ligand.
(34) Balas, L.; Cascio, M. G.; Di Marzo, V.; Durand, T. Synthesis of a potential photoactivatable anandamide analog. *Bioorg. Med. Chem. Lett.* **2006**, *16*, 3765–3768.
(35) Altundas, R.; Mahadevan, A.; Razdan, R. K. A synthetic route to anandamide analogues carrying a substituent at the terminal carbon and an acetylene group in the end pentyl chain. *Tetrahedron Lett.* **2004**, *45*, 5449–5451.
(36) Li, C.; Xu, W.; Vadivel, S. K.; Fan, P.; Makriyannis, A. High affinity electrophilic and photoactivatable covalent endocannabinoid probes for the CB1 receptor. *J. Med. Chem.* **2005**, *48*, 6423–6429.
(37) Dasse, O.; Mahadevan, A.; Han, L.; Martin, B. R.; Marzo, V. D.; Razdan, R. K. The synthesis of *N*-vanillyl-arachidonoyl-amide (arvanil) and its analogs: an improved procedure for the synthesis of the key synthon methyl 14-hydroxy-(all-*cis*)-5.8.11-tetradecatrienoate. *Tetrahedron* **2000**, *56*, 9195–9202.
(38) Caruso, T.; Spinella, A. Cs_2CO_3 promoted coupling reactions for the preparation of skipped diynes. *Tetrahedron* **2003**, *59*, 7787–7790.
(39) Leonard, N. J.; Neelima. 1,1,1,3,3,3-Hexafluoro-2-propanol for the removal of the 4,4′-dimethoxytrityl protecting group from the 5′-hydroxyl of acid-sensitive nucleosides and nucleotides. *Tetrahedron Lett.* **1995**, *36*, 7833–7336.
(40) Bailey, W. J.; Fujiwara, E. Acetylenes. I. Mixed dihalides and halohydrins from butynediol. *J. Am. Chem. Soc.* **1955**, *1*, 165–166.
(41) In our first attempts, there were both side products with over-reduced double bond(s) and compounds with not-yet-reduced alkyne(s) and they migrated with the same R_f (hampered by the presence of amine and boron and/or nickel derivatives salts in the ethanolic reaction mixture). Thus, unfortunately, development and completion of the hydrogenation reaction could not be monitored by hydrogen volume absorption measurement or TLC. We had to use a trial and error approach to find the level of poisoning of the catalyst and reaction time.
(42) Taber, D. F.; Zhang, Z. J. A linpchin approach to unsaturatted fatty acids 11,12-epoxyeicosatrienoic acid and 11*S*,12*S*-dihydroxyeicosatrienoic acid ethyl esters. *Org. Chem.* **2005**, *70*, 8093–8095.
(43) (a) Colonge, J.; Poilane, G. Utilisation du chloro-4 butène-2 ol-1 en synthèse organiqueaction sur les composé organomanesiens. *Bull. Soc. Chim. Fr.* **1955**, *953*, 955. (b) Imai, T.; Nishida, S. A mild and convenient Barbier-type allylation od aldehyddes to homoallylic

alcohol via iodide ion promoted stannylation of allylic bromides and chlorides with tin(II) chloride. *Synthesis* **1993**, *4*, 395–399.

(44) We were mostly preoccupied with double selectivity versus monoselectivity on the dichloride **22**.

(45) Hansen, T. V.; Stenstrom, Y. First total synthesis of (−)-aplyolide A. *Tetrahedron: Asymmetry* **2001**, *12*, 1407–1417.

(46) (a) Kwok, P.-Y.; Muellner, F. W.; Chen, C.-K.; Fried, J. Total synthesis of 7,7-, 10,10-, and 13,13-difluoroarachidonic acids. *J. Am. Chem. Soc.* **1987**, *109*, 3684–3692. (b) Smith, L. M.; Smith, R. G.; Loehr, T. M.; Daves, G. D. Douglas Fir Tusock Moth pheromone: identification of a diene analogue of the principal attractant and synthesis of stereochemically defined 1,6-, 2,6- and 3,6-heneicosadien-11-ones. *J. Org. Chem.* **1978**, *43*, 2361–2366.

(47) Blackburn, C.; Neumeyer, J. L. Receptor-selective fluorescent probes for use in neuroscience. *Med. Chem. Res.* **1992**, *2*, 257–275.

(48) Dohi, H.; Nishida, Y.; Mizuno, M.; Shinkai, M.; Kobayashi, T.; Takeda, T.; Uzawa, H.; Kobayashi, K. Synthesis of an artificial glycoconjugate polymer carrying Pk antigenic trisaccharide and its potent neutralization activity against Shiga-like toxin. *Bioorg. Med. Chem.* **1999**, *7*, 2053–2062.

(49) Perrier, H.; Prasit, P.; Wang, Z. Synthesis of a radioactive photoaffinity arachidonic acid analog. *Tetrahedron Lett.* **1994**, *35*, 1501–1502.

(50) (a) Church, R. F. R.; Conn, R.; Weiss, M. J. Substituted Diaziridines and Diazirines. U.S. Patent 3,525,736 1970; American Cyanamid Compagny. (b) Church, R. F. R.; Weiss, M. J. Diazirines. II. Synthesis and properties of small functionalized diazirine molecules. Some observations on the reaction of a diaziridine with the iodine−iodide ion system. *J. Org. Chem.* **1970**, *35* (8), 2465–2471.

(51) These experiments were run by Pr. Vincenzo DiMarzo team (Napoli) with the same conditions as the ones reported in our preliminary paper (see ref 34).

(52) Grant, D. S.; Kinsella, J. L.; Fridman, R.; Auerbach, R.; Piasecki, B. A.; Yamada, Y.; Zain, M.; Kleinman, H. K. Interaction of endothelial cells with a laminin A chain peptide (SIKVAV) in vitro and induction of angiogenic behavior in vivo. *J. Cell Physiol.* **1992**, *153*, 614–625.

(53) Koch, A. E.; Halloran, M. M.; Haskell, C. J.; Shah; Polverini. Angiogenesis mediated by soluble forms of E-selectin and vascular cell adhesionmolecule-1. *Nature* **1995**, *376*, 517–519.

JM8011382